

PV Cell fed Step-up Resonant Converter for Induction Motor Drive Application

S VANI

M-tech Student Scholar

Department of Electrical & Electronics Engineering,
Visakha Institute of Engineering Technology, Narava,
Visakhapatnam (Dt); Andhra Pradesh, India.
Email:vanisakthimani@gmail.com

B GOPI KRISHNA, MTECH

Assistant Professor

Department of Electrical & Electronics Engineering,
Visakha Institute of Engineering Technology, Narava,
Visakhapatnam (Dt); Andhra Pradesh, India.
Email:

Abstract—In the hybrid micro grid, processes of multiple dc-ac or ac-dc-ac conversions are reduced in an individual ac or dc grid. The hybrid grid consists of both ac and dc networks connected together by multi directional converters. In this micro grid network, it is especially difficult to support the critical load without incessant power supply. The generated power can be extracted under varying wind speed, solar irradiation level and can be stored in batteries at low power demands. In this paper, a hybrid AC-DC micro grid with solar energy, energy storage, and a pulse load is proposed. This micro grid can be viewed as a PEV parking garage power system or a ship's power system that utilizes sustainable energy and is influenced by a pulse load. The battery banks inject or absorb energy on the DC bus to regulate the DC side voltage. The frequency and voltage of the AC side are regulated by a bidirectional AC-DC inverter. The power flow control of these devices serves to increase the system's stability and robustness. The system is simulated in Matlab/Simulink.

F

Index Terms—Renewable energy, resonant converter, soft switching, voltage step-up, voltage stress.

I. INTRODUCTION

In general, manufacturers provide 5 second and ½ an hour surge figures which give an indication of how much power is supplied by the inverter. Solar inverters require a high efficiency rating. Since use of solar cells remains relatively costly, it is paramount to adopt high efficiency inverter to optimize the performance of solar energy system. High reliability helps keep maintenance cost low. Since most solar power stations are built in rural areas without any monitoring manpower, it requires that inverters have competent circuit structure, strict selection of components and protective functions such as internal short circuit protection, overheating protection and overcharge protection. Wider tolerance to DC input current plays an important role, since the terminal voltage varies depending on the load and sunlight [1-4]. Though energy storage batteries are significant in providing consistent power supply, variation in voltage increases as the battery's remaining capacity and internal resistance condition changes especially when the battery is ageing, widening its terminal voltage variation range. In mid-to-

large capacity solar energy systems, inverters' power output should be in the form of sine waves which attain less distortion in energy transmission. Many solar energy power stations are equipped with gadgets that require higher quality of electricity grid which, when connected to the solar systems, requires sine waves to avoid electric harmonic pollution from the public power supply.[5] How Inverters Work: There are three major functions an inverter provides to ensure the operation of a solar system One of the most efficient and promising way to solve this problem is the use of pumping and water treatment systems supplied by photovoltaic (PV) solar energy. Such systems aren't new, and are already used for more than three decades [6-8].

But until recently the majority of the available commercial converters are based on an intermediate storage system performed with the use of batteries or DC motors to drive the water pump. The batteries allow the system to always operate at its rated power even in temporary conditions of low solar radiation [9-10]. This facilitates the coupling of the electric dynamics of the solar panel and the motor used for pumping. Generally, batteries used in this type of system have a low life span, only two years on average, which is extremely low compared to useful life of 15 years of a photovoltaic module. Also, they make the cost of installation and maintenance of such systems substantially high. Furthermore, the lack of batteries replacement is responsible for total failure of such systems in isolated areas this type of system normally uses low-voltage DC motors, thus avoiding a boost stage between the PV module and the motor [11].

Unfortunately, DC motors have low efficiency and high maintenance cost and are not suitable. For such applications the use of a three phase induction motor, due to its high degree of robustness, low cost, higher efficiency and lower maintenance cost compared to other types of motors. These requirements make necessary use of a converter with features high efficiency; low cost; autonomous operation; robustness and high life span [12-13].

II. CONVERTER STRUCTURE AND OPERATION PRINCIPLE

The proposed resonant step-up converter is shown in Fig. 1.

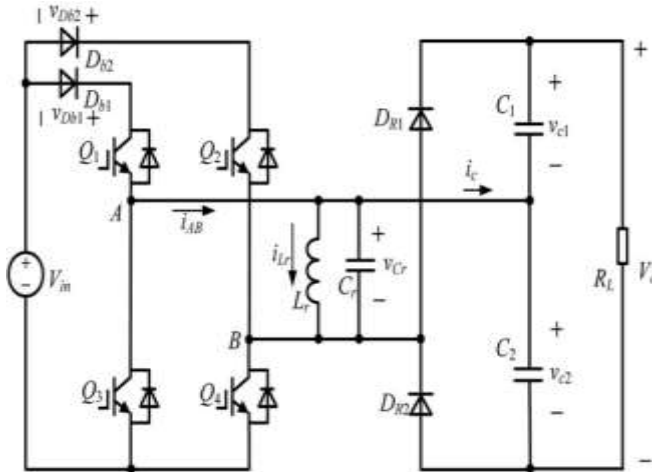


Fig. 1. Topology of the proposed resonant step-up converter.

The converter is composed of an FB switch network, which comprises Q1 through Q4, an LC parallel resonant tank, a voltage doubler rectifier, and two input blocking diodes, Db1 and Db2.

The steady-state operating waveforms are shown in Fig. 2 and detailed operation modes of the proposed converter are shown in Fig. 3. For the proposed converter, Q2 and Q3 are tuned on and off simultaneously; Q1 and Q4 are tuned on and off simultaneously. In order to simplify the analysis of the converter, the following assumptions are made:

- 1) all switches, diodes, inductor, and capacitor are ideal components;
- 2) output filter capacitors C1 and C2 are equal and large enough so that the output voltage Vo is considered constant in a switching period Ts.

A. Mode 1 [t0, t1] [See Fig. 3(a)]

During this mode, Q1 and Q4 are turned on resulting in the positive input voltage Vin across the LC parallel resonant tank, i.e., vLr = vCr = Vin. The converter operates similar to a conventional boost converter and the resonant inductor Lr acts as the boost inductor with the current through it increasing linearly from I0. The load is powered by C1 and C2. At t1, the resonant inductor current iLr reaches I1

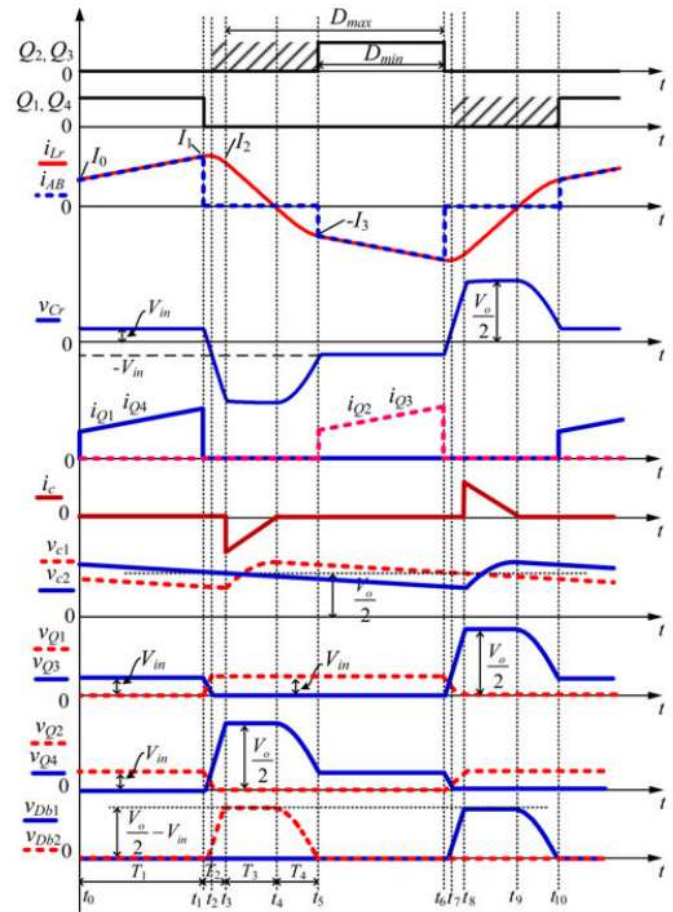


Fig. 2. Operating waveforms of the proposed converter.

$$I_1 = I_0 + \frac{V_{in} T_1}{L_r} \quad (1)$$

Where T1 is the time interval of t0 to t1.

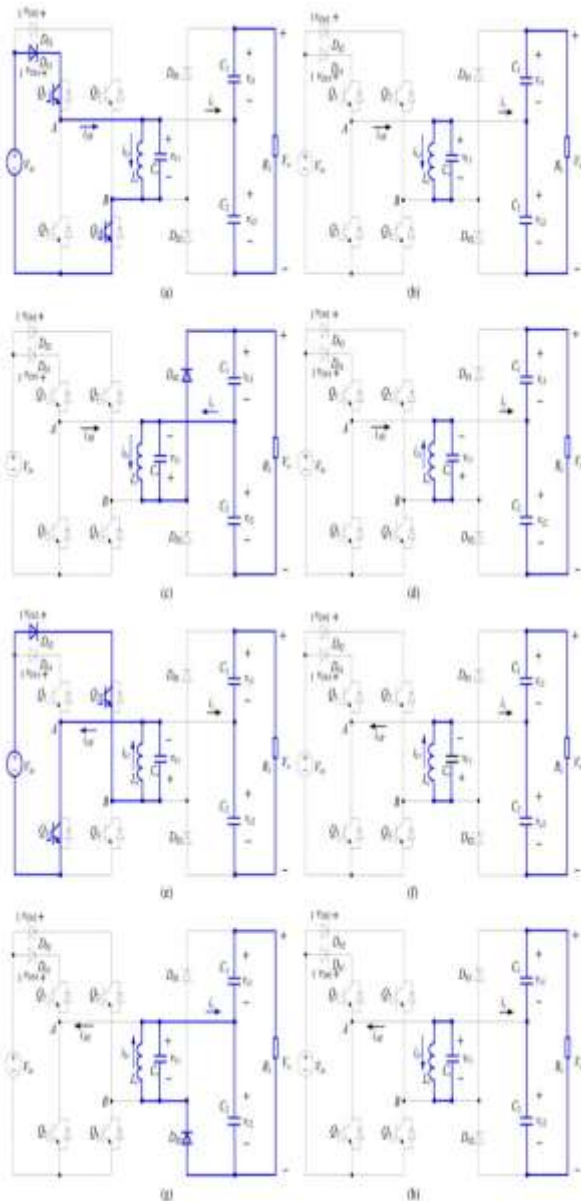


Fig. 3. Equivalent circuits of each operation stages. (a) [t0, t1]. (b) [t1, t3]. (c) [t3, t4]. (d) [t4, t5]. (e) [t5, t6]. (f) [t6, t8]. (g) [t8, t9]. (h) [t9, t10].

In this mode, the energy delivered from V_{in} to L_r is

$$E_{in} = \frac{1}{2} L_r (I_1^2 - I_0^2) \quad (2)$$

B. Mode 2 [t1, t3] [See Fig. 3(b)]

At t1, Q1 and Q4 are turned off and after that L_r resonates with C_r , v_{Cr} decreases from V_{in} , and i_{Lr} increases from I_1 in resonant form. Taking into account the parasitic output

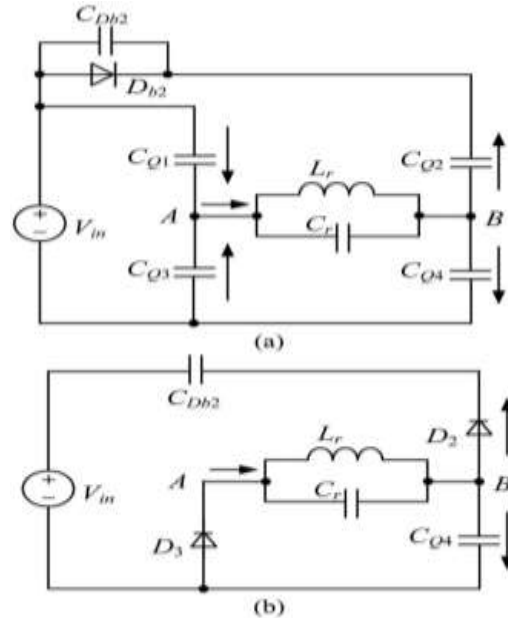


Fig. 4. Further equivalent circuits of Mode 2. (a) [t1, t2]. (b) [t2, t3]. Capacitors of Q1 through Q4 and junction capacitor of Db2, the equivalent circuit of the converter after t1 is shown in Fig. 4(a), in which C_{Db2} , C_{Q1} , and C_{Q4} are charged, C_{Q2} and C_{Q3} are discharged. In order to realize zero-voltage switching (ZVS) for Q2 and Q3, an additional capacitor, whose magnitude is about ten times with respect to C_{Q2} , is connected in parallel with D_{b2} . Hence, the voltage across D_{b2} is considered unchanged during the charging/discharging process and D_{b2} is equivalent to be shorted. Due to C_r is much larger than the parasitic capacitances, the voltages across Q1 and Q4 increase slowly.

As a result, Q1 and Q4 are turned off at almost zero voltage in this mode. When v_{Cr} drops to zero, i_{Lr} reaches its maximum magnitude. After that, v_{Cr} increases in negative direction and i_{Lr} declines in resonant form. At t2, $v_{Cr} = -V_{in}$, the voltages across Q1 and Q4 reach V_{in} , the voltages across Q2 and Q3 fall to zero and the two switches can be turned on under zero-voltage condition. It should be noted that although Q2 and Q3 could be turned on after t2, there are no currents flowing through them. After t2, L_r continues to resonate with C_r , v_{Cr} increases in negative direction from $-V_{in}$, i_{Lr} declines in resonant form. D_{b2} will hold reversed-bias voltage and the voltage across Q4 continues to increase from V_{in} . The voltage across Q1 is kept at V_{in} . The equivalent circuit of the converter after t2 is shown in Fig. 4(b), in which D_2 and D_3 are the antiparallel diodes of Q2 and Q3, respectively. This mode runs until v_{Cr} increases to $-V_o/2$ and i_{Lr} reduces to I_2 , at t3, the voltage across Q4 reaches $V_o/2$ and the voltage across D_{b2} reaches $V_o/2 - V_{in}$. It can be seen that during t1 to t3, no power is

transferred from the input source or to the load, and the whole energy stored in the LC resonant tank is unchanged, i.e.,

$$\frac{1}{2}L_r I_1^2 + \frac{1}{2}C_r V_{in}^2 = \frac{1}{2}L_r I_2^2 + \frac{1}{2}C_r \left(\frac{V_o}{2}\right)^2 \quad (3)$$

We have

$$i_{L_r}(t) = \frac{V_{in}}{Z_r} \sin[\omega_r(t-t_1)] + I_1 \cos[\omega_r(t-t_1)] \quad (4)$$

$$v_{C_r}(t) = V_{in} \cos[\omega_r(t-t_1)] - I_1 Z_r \sin[\omega_r(t-t_1)] \quad (5)$$

$$T_2 = \frac{1}{\omega_r} \left[\arcsin \left(\frac{V_{in}}{\sqrt{V_{in}^2 + \frac{L_r I_1^2}{C_r}}} \right) + \arcsin \left(\frac{V_o}{2\sqrt{V_{in}^2 + \frac{L_r I_1^2}{C_r}}} \right) \right] \quad (6)$$

Where $\omega_r = 1/\sqrt{L_r C_r}$, $Z_r = L_r/C_r$, and T_2 is the time interval of t_1 to t_3 .

C. Mode 3 [t3, t4] [See Fig. 3(c)]

At t_3 , $v_{C_r} = -V_o/2$, DR1 conducts naturally, C1 is charged by i_{L_r} through DR1, v_{C_r} keeps unchanged, and i_{L_r} decreases linearly. At t_4 , $i_{L_r} = 0$. The time interval of t_3 to t_4 is

$$T_3 = \frac{2I_2 L_r}{V_o} \quad (7)$$

The energy delivered to load side in this mode is

$$E_{out} = \frac{V_o I_2 T_3}{4} \quad (8)$$

The energy consumed by the load in half-switching period is

$$E_R = \frac{V_o I_o T_s}{2} \quad (9)$$

Assuming 100% conversion efficiency of the converter and according to the energy conservation rule, in half-switching period

$$E_{in} = E_{out} = E_R \quad (10)$$

Combining (7), (8), (9), and (10), we have

$$I_2 = V_o \sqrt{\frac{I_o T_s}{V_o L_r}} \quad (11)$$

$$T_3 = 2\sqrt{\frac{T_s I_o L_r}{V_o}} \quad (12)$$

D. Mode 4 [t4, t5] [See Fig. 3(d)]

At t_4 , i_{L_r} decreases to zero and the current flowing through DR1 also decreases to zero, and DR1 is turned off with zero-current switching (ZCS); therefore, there is no reverse recovery. After t_4 , L_r resonates with C_r , C_r is discharged through L_r , v_{C_r} increases from $-V_o/2$ in positive direction, and i_{L_r} increases from zero in negative direction. Meanwhile, the voltage across Q4 declines from $V_o/2$. At t_5 , $v_{C_r} = -V_{in}$, and $i_{L_r} = -I_3$. In this mode, the whole energy stored in the LC resonant tank is unchanged, i.e., where T_4 is the time interval of t_4 to t_5 .

$$\frac{1}{2}C_r \left(\frac{V_o}{2}\right)^2 = \frac{1}{2}L_r I_3^2 + \frac{1}{2}C_r V_{in}^2 \quad (13)$$

We have

$$I_0 = I_3 = \frac{1}{2}\sqrt{\frac{C_r(V_o^2 - 4V_{in}^2)}{L_r}} \quad (14)$$

$$i_{L_r}(t) = -\frac{V_o}{2\omega_r L_r} \sin[\omega_r(t-t_5)] \quad (15)$$

$$v_{C_r}(t) = \frac{-V_o \cos[\omega_r(t-t_5)]}{2} \quad (16)$$

$$T_4 = \frac{1}{\omega_r} \arccos \left(\frac{2V_{in}}{V_o} \right) \quad (17)$$

E. Mode 5 [t5, t6] [See Fig. 3(e)]

If Q2 and Q3 are turned on before t_5 , then after t_5 , L_r is charged by V_{in} through Q2 and Q3, i_{L_r} increases in negative direction, and the mode is similar to Mode 1. If Q2 and Q3 are not turned on before t_5 , then after t_5 , L_r will resonate with C_r , the voltage of node A v_A will increase from zero and the voltage of node B v_B will decay from V_{in} ; zero-voltage condition will be lost if Q2 and Q3 are turned on at the moment. Therefore, Q2 and Q3 must be turned on before t_5 to reduce switching loss. The operation modes during $[t_6, t_{10}]$ are similar to Modes 2–4, and the detailed equivalent circuits are shown in Fig. 3(f)–(h). During $[t_6, t_{10}]$, Q2 and Q3 are turned off at almost zero voltage, Q1 and Q4 are turned on with ZVS, and DR2 is turned off with ZCS.

III. A PHOTOVOLTAIC SYSTEM

A photovoltaic system, converts the light received from the sun into electric energy. In this system, semi-conductive materials are used in the construction of

solar cells, which transform the self-contained energy of photons into electricity, when they are exposed to sun light. The cells are placed in an array that is either fixed or moving to keep tracking the sun in order to generate the maximum power [9]. These systems are environmental friendly without any kind of emission, easy to use, with simple designs and it does not require any other fuel than solar light. On the other hand, they need large spaces and the initial cost is high.

PV array are formed by combine no of solar cell in series and in parallel. A simple solar cell equivalent circuit model is shown in figure. To enhance the performance or rating no of cell are combine. Solar cell are connected in series to provide greater output voltage and combined in parallel to increase the current. Hence a particular PV array is the combination of several PV module connected in series and parallel. A module is the combination of no of solar cells connected in series and parallel.

The photovoltaic system converts sunlight directly to electricity without having any disastrous effect on our environment. The basic segment of PV array is PV cell, which is just a simple p-n junction device. The fig.1.4 manifests the equivalent circuit of PV cell. Equivalent circuit has a current source (photocurrent), a diode parallel to it, a resistor in series describing an internal resistance to the flow of current and a shunt resistance which expresses a leakage current. The current supplied to the load can be given as.

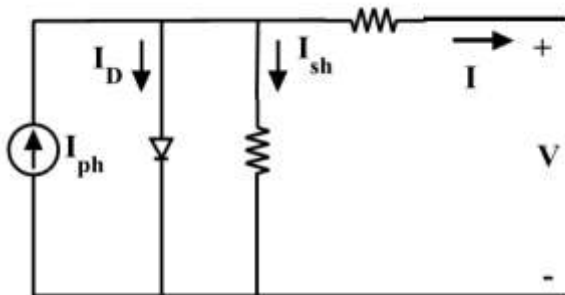


Fig 5 Equivalent circuit of Single diode modal of a solar cell

$$I = I_{PV} - I_0 \left[\exp \left(\frac{V + IR_s}{aV_T} \right) - 1 \right] - \left(\frac{V + IR_s}{R_p} \right)$$

Where

I_{PV} –Photocurrent current,

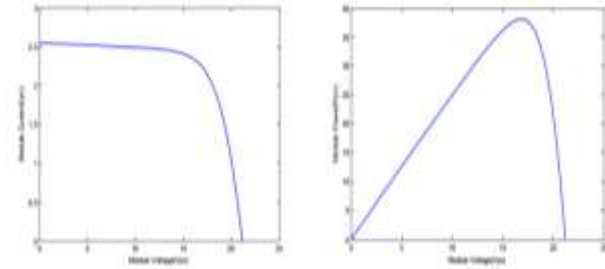
I_0 –diode’s Reverse saturation current,

V –Voltage across the diode,

a – Ideality factor

V_T –Thermal voltage

R_s – Series resistance R_p –Shunt resistance



INDUCTION MOTOR (IM)

An induction motor is an example of asynchronous AC machine, which consists of a stator and a rotor. This motor is widely used because of its strong features and reasonable cost. A sinusoidal voltage is applied to the stator, in the induction motor, which results in an induced electromagnetic field. A current in the rotor is induced due to this field, which creates another field that tries to align with the stator field, causing the rotor to spin. A slip is created between these fields, when a load is applied to the motor. Compared to the synchronous speed, the rotor speed decreases, at higher slip values. The frequency of the stator voltage controls the synchronous speed. The frequency of the voltage is applied to the stator through power electronic devices, which allows the control of the speed of the motor. The research is using techniques, which implement a constant voltage to frequency ratio. Finally, the torque begins to fall when the motor reaches the synchronous speed. Thus, induction motor synchronous speed is defined by following equation,

$$n_s = \frac{120f}{P}$$

Where f is the frequency of AC supply, n , is the speed of rotor; p is the number of poles per phase of the motor. By varying the frequency of control circuit through AC supply, the rotor speed will change.

A. Control Strategy of Induction Motor

Power electronics interface such as three-phase SPWM inverter using constant closed loop Volts / Hertz control scheme is used to control the motor. According to the desired output speed, the amplitude and frequency of the reference (sinusoidal) signals will change. In order to maintain constant magnetic flux in the motor, the ratio of the voltage amplitude to voltage frequency will be kept constant. Hence a closed loop Proportional Integral (PI) controller is implemented to regulate the motor speed to the desired set point. The closed loop speed control is characterized by the measurement of the actual motor speed, which is compared to the reference speed while the

error signal is generated. The magnitude and polarity of the error signal correspond to the difference between the actual and required speed. The PI controller generates the corrected motor stator frequency to compensate for the error, based on the speed error.

IV.MATLAB/SIMULATION RESULTS

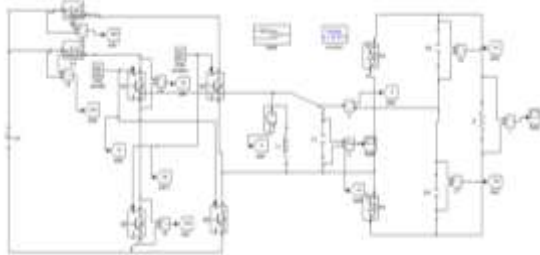


Fig 6 Matlab/simulation circuit of the proposed resonant step-up converter.

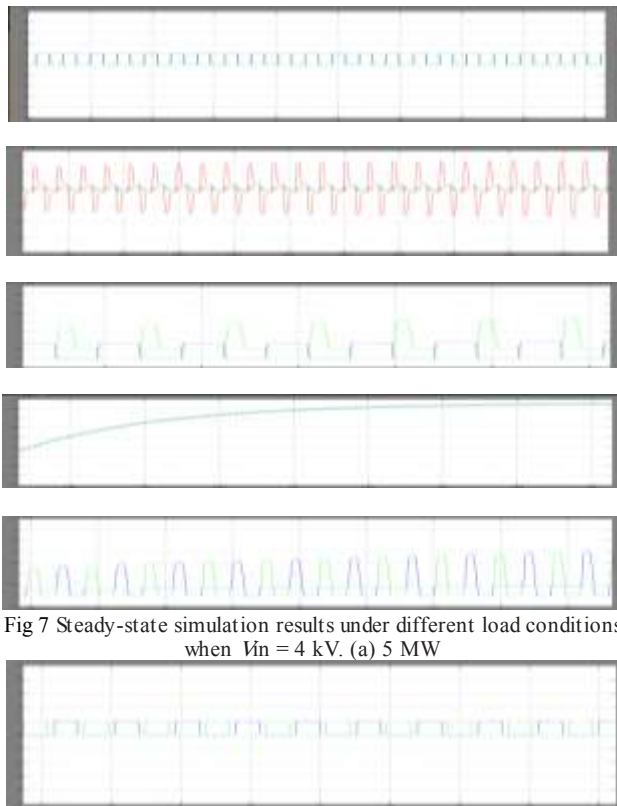


Fig 7 Steady-state simulation results under different load conditions when $V_{in} = 4$ kV. (a) 5 MW

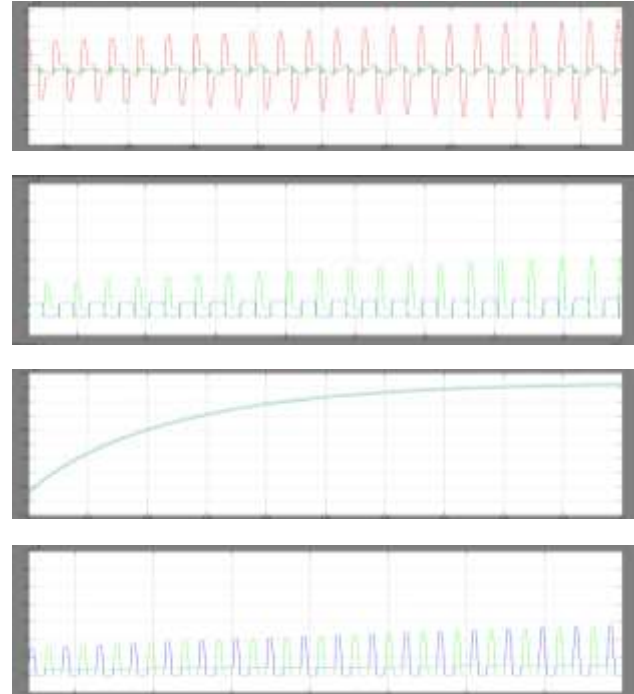


Fig 8 Steady-state simulation results under different load conditions when $V_{in} = 4$ kV. (a) 1 MW.

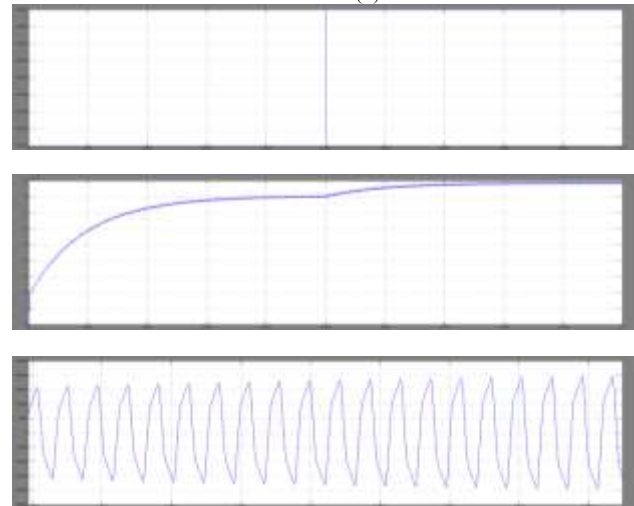
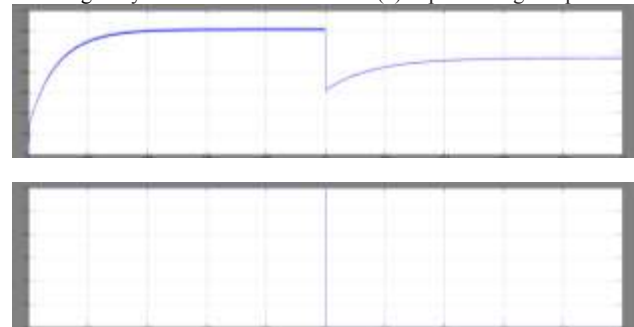


Fig 9 Dynamic simulation results. (a) Input voltage step



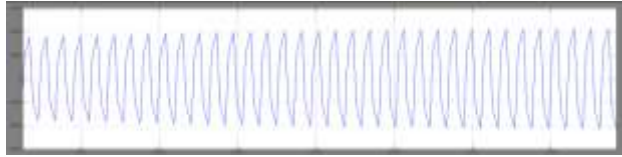


Fig 10 Dynamic simulation results Load step.

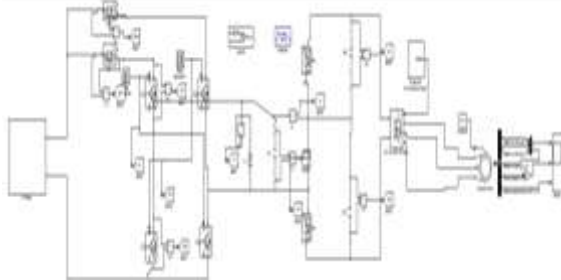


Fig 11 Matlab/simulation circuit of the proposed resonant step-up converter with PV and Induction Motor

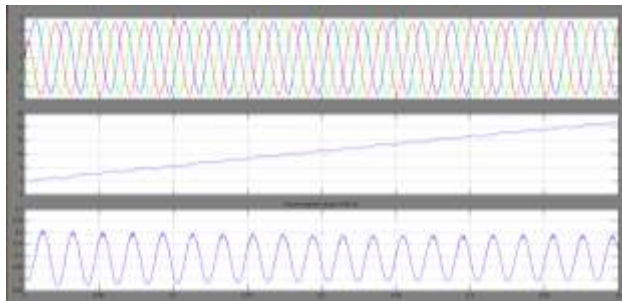


Fig 12 simulation wave form of step-up converter induction motor stator current speed and electromagnetic torque

V. CONCLUSIONS

A novel resonant dc–dc converter is proposed in this paper, which can achieve very high step-up voltage gain and it is suitable for high-power high-voltage applications. The converter utilizes the resonant inductor to deliver power by charging from the input and discharging at the output. The resonant capacitor is employed to achieve zero-voltage turn-on and turn-off for the active switches and ZCS for the rectifier diodes. In this paper, the converter was designed to drive a three phase induction motor directly from PV solar energy and was conceived to be a commercially viable high efficiency, and high robustness.

REFERENCES

- [1] Wu Chen, Member, IEEE, Xiaogang Wu, Liangzhong Yao, Senior Member, IEEE, Wei Jiang, Member, IEEE, and Renjie Hu "A Step-up Resonant Converter for Grid-Connected Renewable Energy Sources" IEEE Transactions On Power Electronics, Vol. 30, No. 6, June 2015.
- [2] CIGRE B4-52 Working Group, HVDC Grid Feasibility Study. Melbourne, Vic., Australia: Int. Council Large Electr. Syst., 2011.
- [3] A. S. Abdel-Khalik, A. M. Massoud, A. A. Elserougi, and S. Ahmed, "Optimum power transmission-based droop control design for multi-terminal HVDC of offshore wind farms," IEEE Trans. Power Syst., vol. 28, no. 3, pp. 3401–3409, Aug. 2013.

[4] F. Deng and Z. Chen, "Design of protective inductors for HVDC transmission line within DC grid offshore wind farms," IEEE Trans. Power Del., vol. 28, no. 1, pp. 75–83, Jan. 2013.

[5] F. Deng and Z. Chen, "Operation and control of a DC-grid offshore wind farm under DC transmission system faults," IEEE Trans. Power Del., vol. 28, no. 1, pp. 1356–1363, Jul. 2013.

[6] C. Meyer, "Key components for future offshore DC grids," Ph.D. dissertation, RWTH Aachen Univ., Aachen, Germany, pp. 9–12, 2007.

[7] W. Chen, A. Huang, S. Lukic, J. Svensson, J. Li, and Z. Wang, "A comparison of medium voltage high power DC/DC converters with high step-up conversion ratio for offshore wind energy systems," in Proc. IEEE Energy Convers. Congr. Expo., 2011, pp. 584–589.

[8] L. Max, "Design and control of a DC collection grid for a wind farm," Ph.D. dissertation, Chalmers Univ. Technol., Goteborg, Sweden, pp. 15–30, 2009.

[9] Y. Zhou, D. Macpherson, W. Blewitt, and D. Jovcic, "Comparison of DCDC converter topologies for offshore wind-farm application," in Proc. Int. Conf. Power Electron. Mach. Drives, 2012, pp. 1–6.

[10] S. Fan, W. Ma, T. C. Lim, and B. W. Williams, "Design and control of a wind energy conversion system based on a resonant dc/dc converter," IET Renew. Power Gener., vol. 7, no. 3, pp. 265–274, 2013.

[11] F. Deng and Z. Chen, "Control of improved full-bridge three-level DC/DC converter for wind turbines in a DC grid," IEEE Trans. Power Electron., vol. 28, no. 1, pp. 314–324, Jan. 2013.

[12] C. Meyer, M. Hoing, A. Peterson, and R. W. De Doncker, "Control and design of DC grids for offshore wind farms," IEEE Trans. Ind. Appl., vol. 43, no. 6, pp. 1475–1482, Nov./Dec. 2007.

[13] C. Meyer and R. W. De Doncker, "Design of a three-phase series resonant converter for offshore DC grids," in Proc. IEEE Ind. Appl. Soc. Conf., 2007, pp. 216–223.